Int. J. Electrochem. Sci., 7 **(2012)** 9004 - 9023

International Journal of
ELECTROCHEMICAL
SCIENCE
www.electrochemsci.org

Thermodynamic, Chemical and Electrochemical Investigations of Calixarene Derivatives as Corrosion Inhibitor for Mild Steel in Hydrochloric Acid Solution

M. Kaddouri[1], *M. Bouklah*[1,2,*], *S. Rekkab*[3], *R. Touzani*[1,4], *S.S. Al-Deyab*[5], *B. Hammouti*[1], *A. Aouniti*[1], *Z. Kabouche*[3]

[1] LCAE-URAC18, Faculté des Sciences, Université Mohammed Premier, B.P. 717, 60000 Oujda, Morocco
[2] Laboratoire de Physico-chimie des Matériaux, Centre Régionale des Métiers de l'Education et de Formation "CRMEF", Académie Régionale de l'Orientale, Oujda, Morocco
[3] Laboratoire d'Obtention de Substances Thérapeutiques, Université Mentouri-Constantine, 25000 Constantine, Algérie
[4] Université Mohammed Premier Faculté Pluridisciplinaire de Nador
[5] Petrochemical Research Chair, Department of Chemistry - College of Science, King Saud University, B.O. 2455 Riaydh 11451Saudi Arabia.
[*]E-mail: hammoutib@gmail.com

Received: 29 July 2012 / *Accepted:* 14 August 2012 / *Published:* 1 September 2012

The focus of this study is to synthesize new calixarene derivatives namely calix[8]arenes (3a) (P1) and (2a) (P2), and to test its performance as corrosion inhibitor of steel in molar HCl at 308K. Polarization and weight loss measurements were used. The inhibition efficiency was found to increase with calixarene derivatives content to attain 95.14% for (P1) and 80% for (P2) at 10^{-3}M. Polarization curves revealed that calixarene derivatives affect both cathodic and anodic domains by decreasing current densities and then it may be classified was mixed type inhibitors. The calixarene derivatives tested is adsorbed on the surface according to the Langmuir adsorption isotherm. Free enthalpy of adsorption reveals that calixarene derivatives act from physisorption onto the steel surface.

Keywords: Corrosion; Steel; Calixarene; Inhibition; Hydrochloric acid; Thermodynamic.

1. INTRODUCTION

Steel is extensively used in various industrial operations and the study of its corrosion inhibition in pickling bath is of great importance. The use of inhibitors is one of the practical methods for protection against corrosion in especially acidic media [1-3]. Most of the effective inhibitors are

organic compounds combining nitrogen, oxygen, phosphorous and sulphur in their structures [4-10].The inhibiting actions of organic compounds are usually attributed to their interactions with the metal surface via their adsorption. These compounds in general are adsorbed on the metal surface, blocking the active corrosion sites. Four types of adsorption may take place by organic molecules at metal/solution interface: (1) electrostatic attraction between the charged molecules and the charged metal, (2) interaction of unshared electron pairs in the molecule with the metal, (3) interaction of π electrons with the metal and (4) combination of (1) and (3) [11]. The adsorption ability of inhibitors onto metal surface depends on the nature and surface charge of metal, the chemical composition of electrolytes, and the molecular structure and electronic characteristics of inhibitor molecules. Organic compounds containing functional electronegative groups and π electrons in triple or conjugated double bonds are usually good inhibitors [12-14]. Calixarenes are macrocyclic compounds made of phenolic units linked together by methylene bridges [15-17]. They can be functionalized on the upper (the para position) and lower (the OH groups) rims [15-17]. Calixarenes can exist in several conformations: cone, partial cone, 1,2-alternate and 1,3-alternate [15-17]. The complexing properties of calixarenes are depending on their conformation and the functionalities attached to the central core. Thus, due to the numerous possibilities in functionalization associated to the conformations, they offer a large panel of ligands useful in different fields of research: chemistry, cosmetology, environmental technologies, etc [18, 19]. They are investigated as ion-carriers through liquid membranes [20-22]. They are used in the treatment of waste waters notably concerning the uranium [20, 21, 23, 24]. Similarly, they are used for decontamination of used waters that is for the removal of toxic cations such as cesium, lanthanides, and actinides or to neutralized undesired pollutants [20-21, 23-24].

The encouraging results obtained by very similar calixarenes have incited us to plane new route in synthesis of new calixarene derivatives which may play determinant role in hinder corrosion to reasonable level [25-27].

This paper is aimed to synthesize a new calyx and to study its application as corrosion inhibitor of steel in hydrochloric acid solution. This later investigation is conducted by gravimetric, polarization method and EIS techniques.

2. EXPERIMENTAL PART

2.1. Chemistry

The treatment of the calix[8]arenes **(1a-b)** with 1,3-propane sultone, during three days at room temperature, led to the new corresponding water-soluble calix[8]arenes **(2a-b)** bearing a propane sulfonic group with excellent yields (98 and 95%, respectively). The reaction of **(1a-b)** with a pyrane sultone afforded, after four days, two new calix[8]arenes bearing a butane sulfonic group **(3a)** in 86 and 98% yields, respectively (scheme 1).

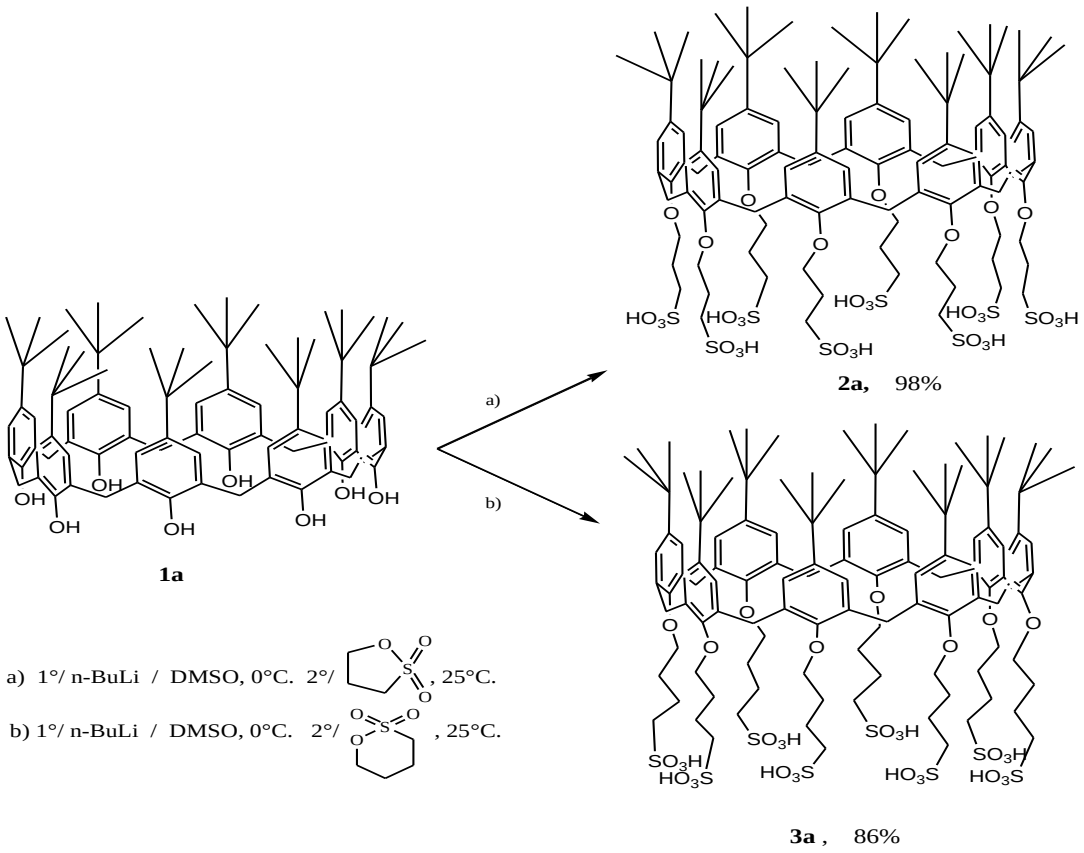

Scheme 1. Synthesis of new water soluble sulfonated calix[8]arenes **3a** (P1)and **2a** (P2)

The *in situ* produced phenolate from n-BuLi in DMSO reacts with the sultone through a ring opening reaction (scheme 2). The reaction was controled by ^{1}NMR spectroscopy and the products were purified by recristallization in ethanol.

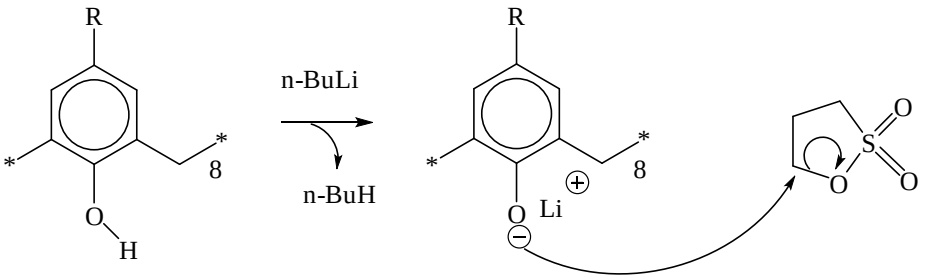

Scheme 2. Possible pathway of the reaction with the sultone.

The ^{1}HNMR spectra of (**2b**) exhibited three multiplets at 3.17, 1.96, 1.37, ppm corresponding to the resonance of CH_2O, CH_2SO_3 and C-CH_2-CH groups, respectively. The IR spectra showed the appearence of the new bands at 3207 cm^{-1} (OH), 2935 cm^{-1} (-CH_2), 2877 cm^{-1} (Ar-H), 1448 cm^{-1} (Ar-CH_2), 1186 cm^{-1} (CH_2O) and 1051 cm^{-1} (S=O). The mass spectra showed a molecular ion at m/z: 1824.37 corresponding to the $C_{80}H_{96}O_{32}S_8$ formula.

The ^{1}HNMR spectra of (**3b**) was characterized by the presence of three multiplets at 3.71, 2.35, 1.73 ppm attributed to CH_2O, CH_2SO_3, C-CH_2-CH_2-CH groups, respectively. ES/MS shows a molecular ion at m/z: 1937.49 corresponding to the $C_{88}H_{112}O_{32}S_8$ formula.

2.2. Material preparation

Corrosion tests have been carried out on electrodes cut from sheets of mild steel. Steel containing 0.09% P, 0.38% Si, 0.01% Al, 0.05% Mn, 0.21% C, 0.05% S and the remainder iron were used for the measurement of weight loss and electrochemical studies. The surface preparation of the specimens was carried out using emery paper nos. 260, 400 and 1200; they were degreased with AR grade ethanol, acetone and dried at room temperature before use. The solutions (1M HCl) were prepared by dilution of an analytical reagent grade 37% HCl with doubly distilled water. The solubility of the tested some sulphuric compounds are about 10^{-3} M in 1M HCl.

2.3. Gravimetric measurements

For weight loss measurements, each run was carried out in a double walled glass cell equipped with a thermostat-cooling condenser containing 100 ml test solution. The steel specimens used had a rectangular form (1.5 ×1. 5 × 0.05 cm), was completely immersed at inclined position in the vessel. The immersion time for the weight loss was 6h at 308K. After 6 h of immersion, the electrode was withdrawn, rinsed with doubly distilled water, washed with ethanol, dried and weighed. Duplicate experiments were performed in each case and the mean value of the weight loss has been reported. The weight loss was used to calculate the corrosion rate (W) in milligrams per square centimetre per hour (mg/cm^2 h).

2.4. Polarisation measurements

Electrochemical measurements were carried out in conventional three- electrode cylindrical Pyrex glass cell. The working electrode was a disc cut from iron (99.5% purity) sheet. The exposed area to the corrosive solution was 1 cm^2. A platinum electrode and saturated calomel electrode (SCE) were used, respectively, as auxiliary and reference electrodes. All potentials are given in the SCE scale. The cell was thermostated at 308K.

The polarisation curves were recorded with a potentiostat type AMEL 550 using a linear sweep generator type AMEL 567 at scan rate of 30mV/min. Before recording the cathodic potentiokinetic curves up the corrosion potential, the iron electrode was polarised at 800 mV/SCE for 10min.

However, for anodic polarisation curves, the potential of the working electrode was swept from its open circuit potential value after 30 min at rest. Solutions were de-aerated with nitrogen. The nitrogen bubbling was maintained in the solutions during the electrode chemical measurements.

2.5. Electrochemical impedance spectroscopy (EIS)

The electrochemical impedance spectroscopy (EIS) measurements were carried out with the electrochemical system (Tacussel) which included a digital potentiostat model Voltalab PGZ 100 computer at E_{corr} after immersion in solution without bubbling, the circular surface of steel exposing of 1 cm^2 to the solution were used as working electrode. After the determination of steady-state current at a given potential, sine wave voltage (10 mV) peak to peak, at frequencies between 100 kHz and 10 MHz were superimposed on the rest potential. Computer programs automatically controlled the measurements performed at rest potentials after 30 min of exposure. The impedance diagrams are given in the Nyquist representation.

3. RESULTS AND DISCUSSION

3.1. Weight loss measurements

The corrosion of mild steel in 1M HCl medium containing various concentrations of sulphuric componds was studied by weight loss measurements. In this case, *E* (%) is calculated by applying the following equation:

$$E\% = \left[\frac{W_{corr} - W_{corr'inh)}}{W_{corr}} \right] \times 100 \qquad (1)$$

where W_{corr} and $W_{corr(inh)}$ are the corrosion rates of mild steel in the absence and presence of inhibitor molecule, respectively. Table 1 summarizes the corrosion rates (*W*) of mild steel and the *E* (%) for some inhibitors studied at different concentrations. It is obvious from these data that all of these compounds inhibit the corrosion of mild steel in 1M HCl solution at all concentrations used in this study and the corrosion rate was seen to decrease with increasing additive concentration at 35°C. At 10^{-3} M, *E* (%) attains 95.14% for P1. Thus, we deduce that this inhibitor is the better inhibitor for the mild steel and *E* (%) was found to be in the following order: P1> P2. The difference in their inhibitive action can be explained on the effect of chain length. We cite in the same context (work of Natalya et al. 2011). They study the effect of chain length of imidazolium-type ionic liquids [28]. As a result of this classification and in order to better understand the inhibition mechanism of organic compounds studied, a detailed study using electrochemical polarisation was carried out.

The inhibition efficiencies obtained can be explained by the length and the nature of the carbonic chain joining the cycle, the rise of the inhibition efficiency is due to the inductive effect of the methyl, ethyl and t-Bu groups.

Table 1. Corrosion parameters obtained from weight loss of mild steel in 1M HCl containing various concentrations of calixarene derivatives at 308K.

Inhibitors	C(M)	W(mg/cm^2.h)	E_w (%)	Θ
Blank	1	9.003	-	-
P1	10^{-3}	0.4371	95.14	0.9514
	5×10^{-4}	1.188	86.80	0.8680
	10^{-4}	3.217	65.00	0.6500
	5×10^{-5}	3.315	63.00	0.6300
	10^{-5}	3.725	59.00	0.5900
	10^{-6}	3.701	58.00	0.5800
P2	10^{-3}	1.814	80.00	0.8000
	5×10^{-4}	3.660	60.00	0.600
	10^{-4}	4.262	53.00	0.5300
	5×10^{-5}	5.256	52.00	0.5200
	10^{-5}	4.720	48.00	0.4800
	10^{-6}	5.860	35.00	0.3500

3.2. Potentiodynamic polarisation

Fig. 1 shows the cathodic and anodic polarisation curves of mild steel in 1M HCl blank solution and in the presence of different concentrations (10^{-3} to 10^{-6} M) of inhibitors studied. With the increase of organic compounds concentrations, both anodic and cathodic currents were inhibited. This result shows that the addition of inhibitor reduces anodic dissolution and retards the hydrogen evolution reaction.

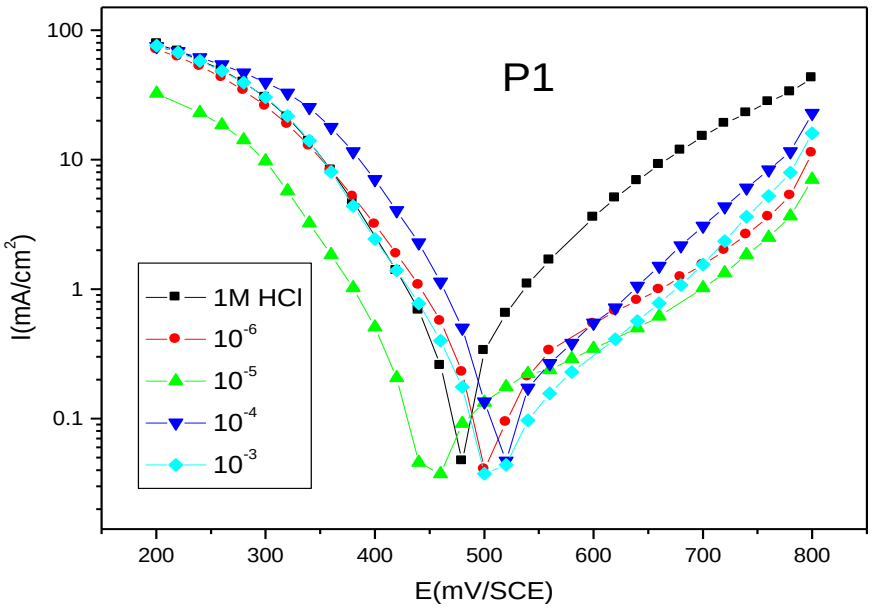

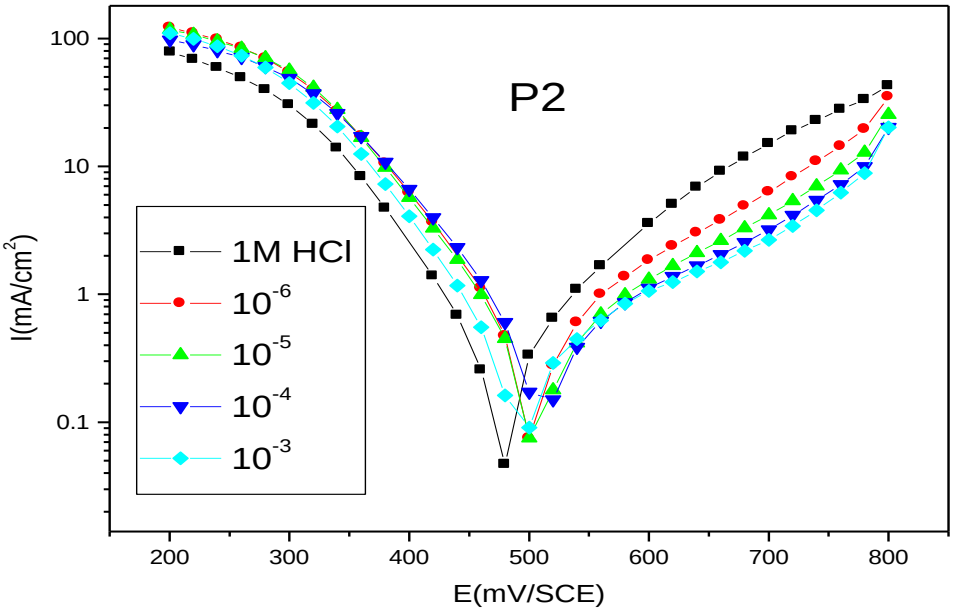

Figure 1. Polarisation curves for C38 steel in 1M HCl containing different concentrations of inhibitors studied at 308K.

Table 2 gives the values of kinetic corrosion parameters as the corrosion potential E_{corr}, corrosion current density I_{corr}, Tafel slope b_c, and inhibition efficiency for the corrosion of mild steel in 1M HCl with different concentrations of inhibitor.

The inhibition efficiency E_I is obtained by:

$$E_I = 100 \times \left(1 - \frac{I_{corr}}{I^{\circ}_{corr}}\right) \qquad (2)$$

I_{corr} and I°_{corr} are the corrosion current density values with and without the inhibitor, respectively, determined by extrapolation of cathodic Tafel lines to corrosion potential.

Table 2. Potentiodynamic polarisation parameters for corrosion of carbon steel in 1M HCl with various concentrations of inhibitor at 308K.

Inhibitor	C(M)	E_{corr} (mV)	b_c (mV/ dec)	b_a (mV/ dec)	I_{corr} ($\mu A/cm^2$)	E%
P1	HCl 1M	-478	-152	78.7	0.5735	--
	10^{-3}M	-512	-117	47.6	0.0374	**93.5**
	10^{-4}M	-514	-127	51.9	0.1068	**81.4**
	10^{-5}M	-451	-385	82.2	0.1474	**74.3**
	10^{-6}M	-507	-206	84.8	0.177	**69.1**
P2	10^{-3}M	-493	-233	84.4	0.3385	**40.1**
	10^{-4}M	-511	-210	93	0.396	**31**
	10^{-5}M	-506	-200	92	0.448	**21.8**
	10^{-6}M	**-504**	**-183**	**95**	**0.533**	**7**

From Table 2, it can be concluded that:

• The I_{corr} values decrease with increasing inhibitor concentration.

• The addition of some compounds produces slight changes in the values of E_{corr} and b_c. This indicates [29] that the adsorbed molecules of inhibitor do not affect the mechanism of hydrogen evolution.

• The values of inhibition efficiency *(E*%) increase with inhibitor concentration reaching a maximum value (93.5%) at 10^{-3} M.

• The calixarene derivatives were mixed inhibitors.

3.3. Electrochemical impedance spectroscopy measurements

The corrosion behaviour of steel, in acidic solution in the presence of P1 and P2 at different concentrations was investigated by EIS measurements at room temperature.

As observed, the Nyquist plots contain a depressed semi-circle with the center below the real X-axis, which is size increased by increasing the inhibitor concentrations, indicating that the corrosion is mainly a charge transfer process [30] and the formed inhibitive film was strengthened by the addition of calixarene compounds . The depressed semi-circle is the characteristic of solid electrodes and often refers to the frequency dispersion which arises due to the roughness and other inhomogeneities of the surface [31]. It is worth noting that the change in concentration of calixarene copounds did not alter the style of the impedance curves, suggesting a similar mechanism of the inhibition is involved.

Nyquist plots of steel in inhibited and uninhibited acidic solutions containing various concentrations of sulphuric compounds are shown in Fig.2.

The charge-transfer resistance (R_t) values are calculated from the difference in impedance at lower and higher frequencies. To obtain the double layer capacitance (C_{dl}) the frequency at which the imaginary component of the impedance is maximal ($-Z_{max}$) is found as represented in equation.

$$C_{dl} = \frac{1}{\omega . R_t} \quad \text{Where} \quad \omega = 2\pi f_{max} \qquad (3)$$

The inhibition efficiency obtained from the charge transfer resistance is calculated by:

$$E(\%) = \frac{\left[R_{t/inh} - R_t \right]}{R_{t/inh}} .100 \qquad (4)$$

R_t and $R_{t/inh}$ are the charge transfer-resistance values with and without inhibitor, respectively.

The charge transfer resistance, R_t, the double layer capacitance C_{dl}, the frequency f_{max} values were given in Table3.

The obtaining of the semicircle in the impedance diagrams indicated that the corrosion of steel is controlled by a charge transfer process. Table 3 shows the impedance parameters obtained by line fitting to the semicircle. The charge transfer resistance (R_t) increases with the inhibitor concentration. Also, the double layer capacitance (C_{dl}) decreases with increase in the concentration of the inhibitor. This decrease is due to the adsorption of the inhibitor at the metal surface causing a change of the double layer structure [32]. When comparing the inhibition efficiencies obtained from testing methods used in this study, it can be concluded that there is a fair agreement between results obtained by different techniques used.

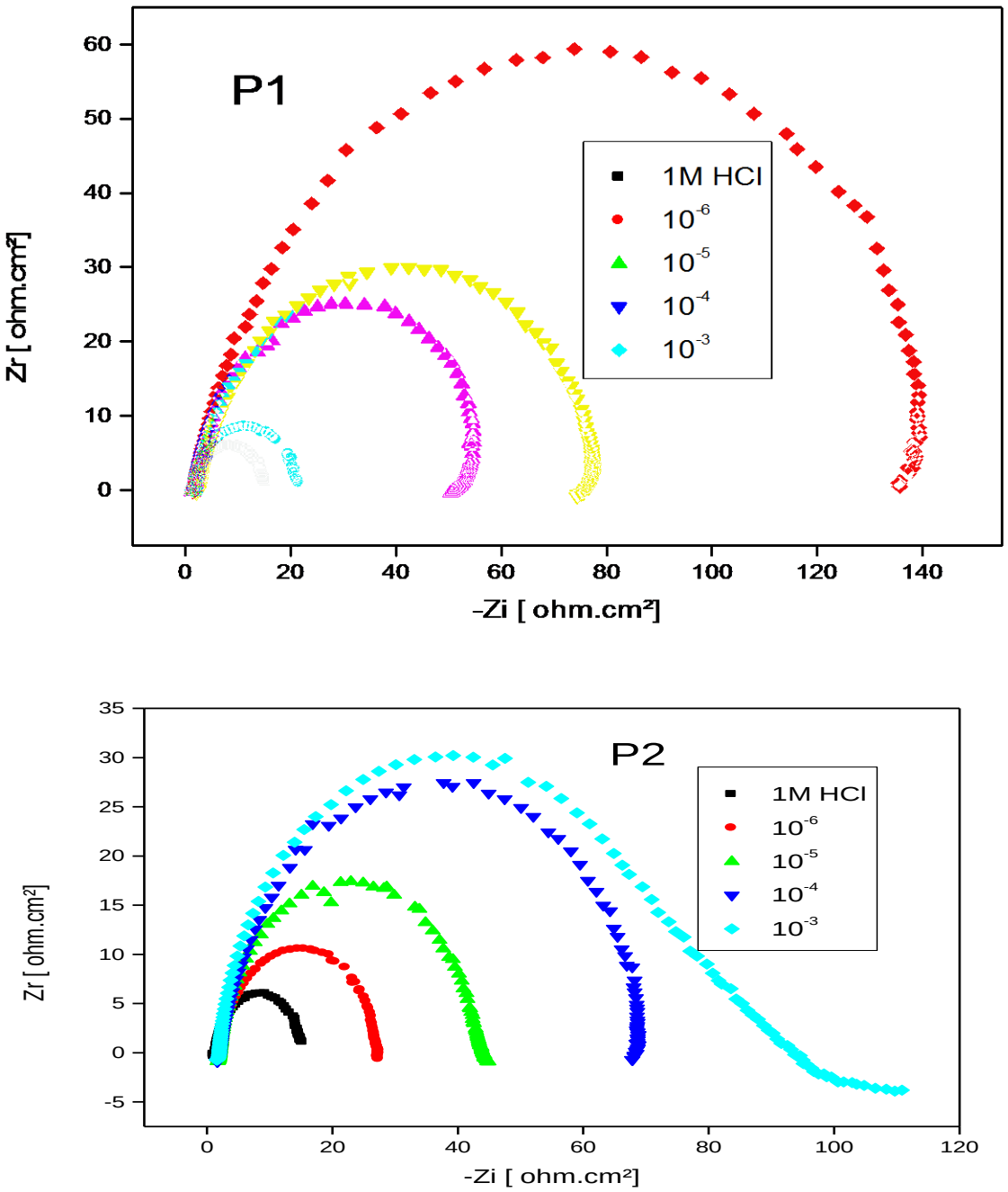

Figure 2. Nyquist diagrams for steel in 1M HCl with different concentrations of P1 and P2

Table 3. Parameters corresponding to the Nyquist plots of the impedance data for steel in 1M HCl for various concentrations of P1 and P2.

Inhibitor	concentration	R_t / Ω cm^2	F_{max} / Hz	C_{dl} / µF cm^{-2}	E / %
P1	HCl(1M)	20	113.7	70	**--**
	10^{-6}M	30	82.53	64.28	**33.33**
	10^{-5}M	60	50.76	52.25	**66.66**
	10^{-4}M	80	38.60	51.53	**75.00**
	10^{-3}M	140	22.54	50.42	**85.71**
P2	10^{-6}M	27	111.51	52.86	**44.44**
	10^{-5}M	45	70.24	50.35	**66.66**
	10^{-4}M	70	47.89	47.47	**78.57**
	10^{-3}M	**100**	**51.12**	**31.13**	**85.00**

3.4. Effect of temperature

In order to study the effect of temperature on the inhibition efficiencies of calixarenes derivatives, weight loss measurements were carried out in the temperature range 318–348K in absence and presence of inhibitors at different concentration. The various corrosion parameters obtained are listed in Table 4.

Table 4. Effect of temperature on the corrosion rate of steel in 1M HCl (W_0) without and with P1and P2 at 10^{-3} to 10^{-6} M and the corresponding corrosion inhibition efficiency.

Inhibitor	T (K)	C (M)	W (mg/cm^2.h)	E %	θ
P1	318	blank 1M	1.908	-	
		10^{-3}	0.1908	90.00	0.9000
		10^{-4}	0.3968	79.20	0.7920
		10^{-5}	0.5127	73.00	0.7300
		10^{-6}	0.7441	61.01	0.6101
	328	blank 1M	2.092	-	
		10^{-3}	0.3974	81.00	0.8100
		10^{-4}	0.7696	63.21	0.6321
		10^{-5}	0.8466	59.53	0.5953
		10^{-6}	0.8781	58.02	0.5802
	338	blank 1M	3.890	-	
		10^{-3}	1.168	70.00	0.7000
		10^{-4}	1.671	57.04	0.5704
		10^{-5}	2.742	42.05	0.4205
		10^{-6}	2.254	29.50	0.2950
	348	blank 1M	8.744	-	
		10^{-3}	4.422	49.00	0.4900
		10^{-4}	5.430	38.00	0.3800
		10^{-5}	6.010	31.00	0.3100
		10^{-6}	7.107	18.00	0.1800

Inhibitor	T (K)	C(M)	W (mg/cm^2.h)	E %	θ
P2	318	blank 1M	1.908	-	
		10^{-3}	0.5504	71.15	0.7115
		10^{-4}	0.9442	50.51	0.5051
		10^{-5}	1.169	38.73	0.3873
		10^{-6}	1.377	27.80	0.2780
	328	blank 1M	2.092	-	
		10^{-3}	0.694	66.81	0.6681
		10^{-4}	1.123	46.31	0.4631
		10^{-5}	1.421	32.03	0.3203
		10^{-6}	1.660	20.18	0.2018
	338	blank 1M	3.890	-	
		10^{-3}	1.790	54.00	0.5400
		10^{-4}	2.440	37.35	0.3735
		10^{-5}	2.873	26.12	0.2612
		10^{-6}	3.320	14.43	0.1443
	348	blank 1M	8.744	-	
		10^{-3}	4.802	45.08	0.4508
		10^{-4}	6.281	28.16	0.2816
		10^{-5}	7.067	19.17	0.1917
		10^{-6}	8.041	08.03	0.0803

Inspection of Table 4 showed that corrosion rate increased with increasing temperature both in uninhibited and inhibited solutions while the inhibition efficiency of calexarene derivatives decreased with temperature. A decrease in inhibition efficiencies with the increase temperature in presence of calexarene derivatives might be due to weakening of physical adsorption.

In order to calculate activation parameters for the corrosion process, Arrhenius Eq. (5) and transition state Eq. (6) were used [33]:

$$W = A\exp\left(-\frac{E_a}{RT}\right) \qquad (5)$$

$$W = \frac{RT}{Nh}\exp\left(\frac{\Delta S_a^o}{R}\right)\exp\left(-\frac{\Delta H_a^o}{RT}\right) \qquad (6)$$

Where W is the corrosion rate, R the gas constant, T the absolute temperature, A the pre-exponential factor, h the Plank's constant and N is Avogadro's number, E_a the activation energy for corrosion process , ΔH_a° the enthalpy of activation and ΔS_a° the entropy of activation.

The apparent activation energy (E_a) at different concentration of calixarene derivatives was determined by linear regression between Ln W and 1/T (Fig. 3) and the result is shown in Table 5.

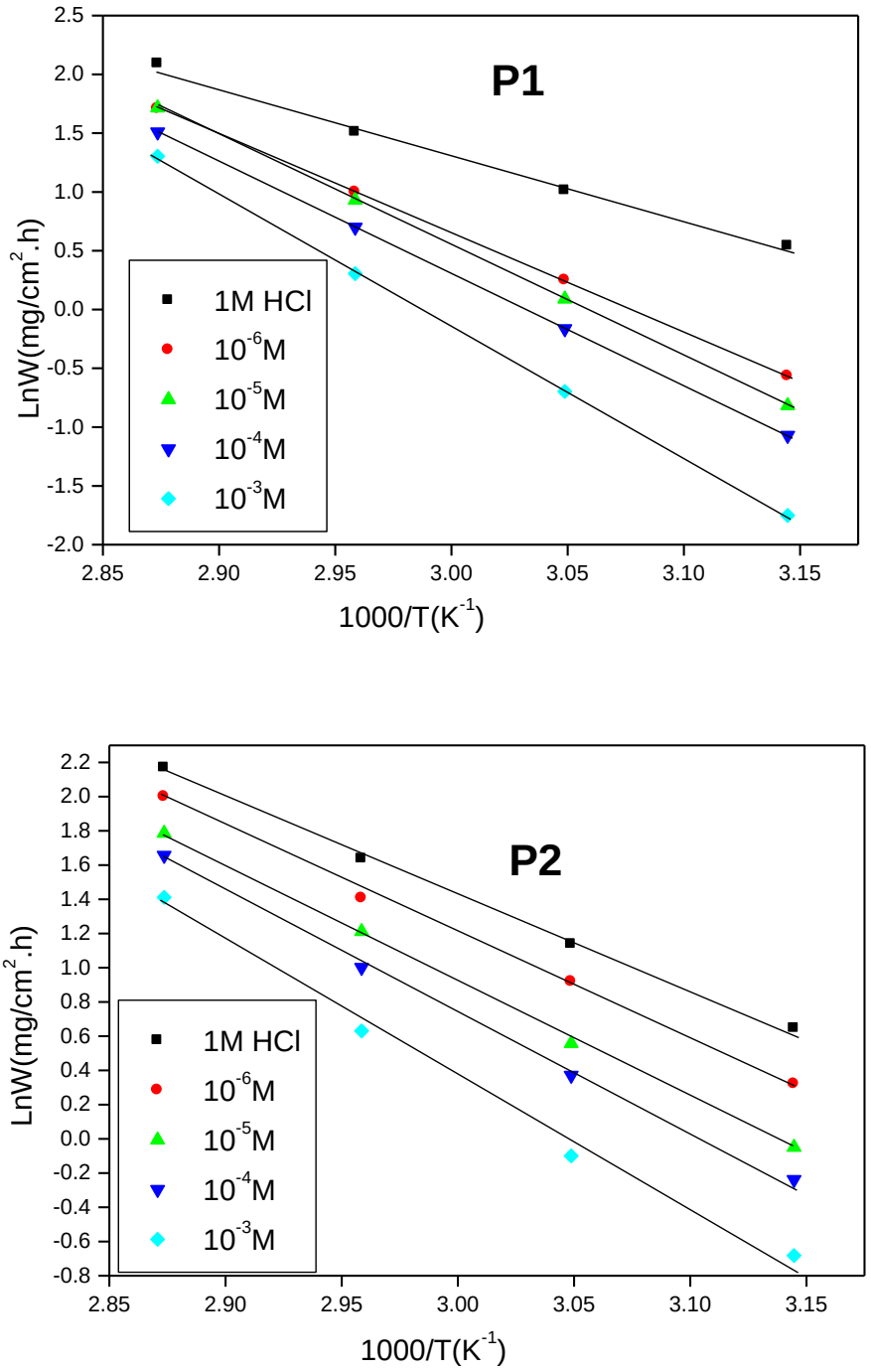

Figure 3. Arrhenius plots for steel in 1M HCl in the absence and presence of P1 and P2

The linear regression coefficient was close to 1, indicating that the steel corrosion in 1M HCl acid can be elucidated using the kinetic model. Inspection of Table 5 showed that the value of E_a determined in 1M HCl containing inhibitors is higher than that for uninhibited solution. The increase in the apparent activation energy may be interpreted as physical adsorption that occurs in the first stage [34]. This suggests a similar inhibition mechanism for the inhibitors. The increase in Ea in case of the protected steel with the addition the inhibitors of different concentration indicates that the energy

barrier for the corrosion reaction increases. The increase in Ea of the corrosion process could be attributed to the adsorption of the inhibitor molecules onto the metal surface which decreases the interaction between the corrosive medium and the metal surface.

Table 5. The values of activation parameters E_a, ΔH_a^0 and ΔS_a^0 for mild steel in 1M HCl in the absence and the presence of different concentrations of P1 and P2.

	C (M)	E_a (kJ mol^{-1})	ΔH_a^0 (kJ mol^{-1})	ΔS_a^0 (J mol^{-1} K^{-1})	Ea-ΔH_a (kJ mol^{-1})
	Blank	47.11	44.56	-45.88	2.55
P1	10^{-6} M	70.42	67.66	18.84	2.76
	10^{-5} M	78.60	75.86	42.64	2.74
	10^{-4} M	79.07	76.31	42.08	2.76
	10^{-3} M	96.31	93.53	89.85	2.78
P2	Blank	47.33	44.57	-101.84	2.76
	10^{-6} M	54.70	51.99	-37.70	2.76
	10^{-5} M	55.75	53.00	-13.85	2.75
	10^{-4} M	59.02	56.25	-14.47	2.77
	10^{-3} M	68.09	65.35	33.23	2.74

Fig. 4 shows a plot of ln (W /T) against 1/T in the absence and presence of the inhibitors. A straight lines are obtained with a slope of ($-\Delta H_a^0/R$) and an intercept of (Ln $R/Nh + \Delta S_a^0/R$) from which the values of ΔH_a^0 and ΔS_a^0 are calculated, are listed in Table 5. The relationship between the activation energy E_a and activation heat ΔH_a^0 against the concentration of inhibitors P1 and P2 is shown in Fig. 5. From the data obtained in Table 5, it seems that E_a and ΔH_a^0 vary in the same manner, these results agree those obtained in the literature [35] this result allows verification of the known thermodynamic reaction between the E_a and ΔH_a^0 :

$$\Delta H_a^0 = E_a - RT \qquad (7)$$

The positive signs of the enthalpies (ΔH_a^0) reflect the endothermic nature of the steel dissolution process (Table 5). The entropy of activation ΔS_a^0 in the absence of inhibitor is negative and this value increases positively with the P1. The increase of ΔS_a^0 implies that an increase in disordering takes place on going from reactants to the activated complex [36]. For P2 large and negative values of entropies (ΔS_a^0) imply that the activated complex in the rate determining step represents an association rather than a dissociation step, meaning that a decrease in disordering takes place on going from reactants to the activated complex [37].

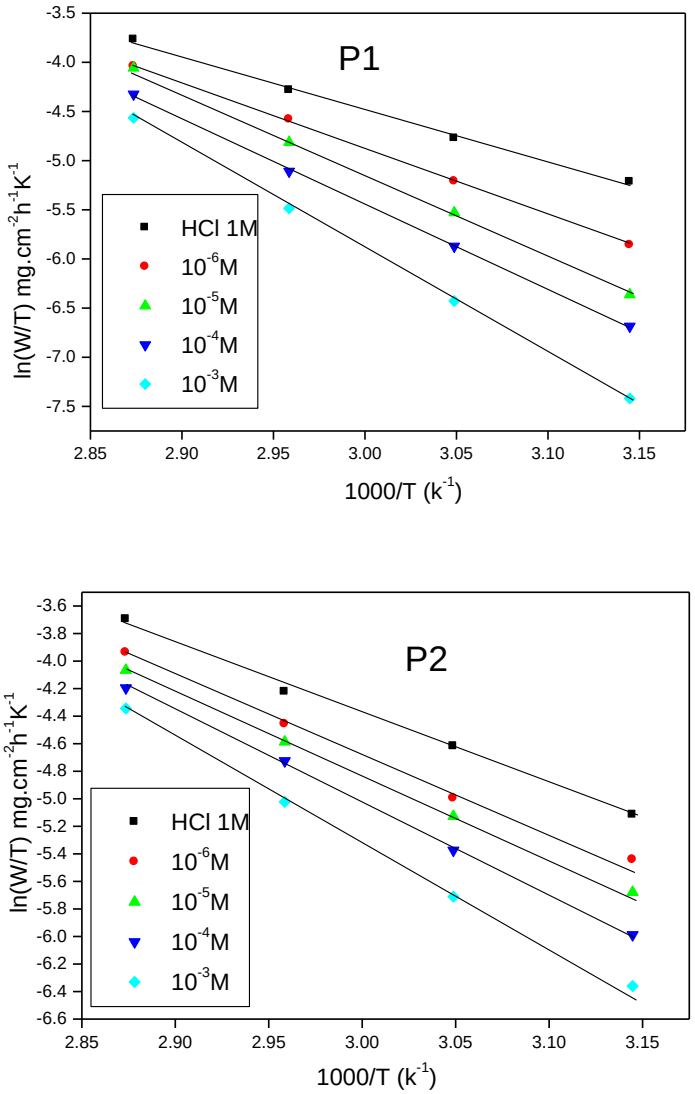

Figure 4. Arrhenius plots of ln (*W*/*T*) versus 1/*T* at different concentrations of P1and P2.

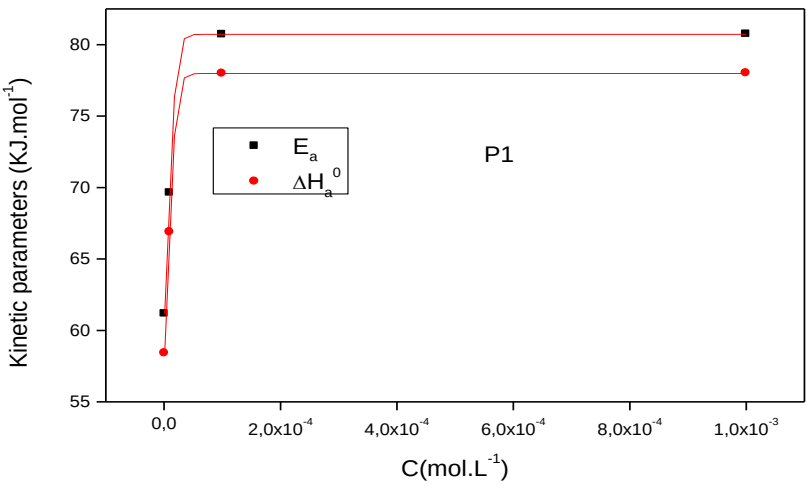

Figure 5. Variation of E_a and ΔH_a^0 versus concentration of inhibitor P1

3.5 Adsorption isotherm and thermodynamic parameters

Assuming the corrosion inhibition was caused by the adsorption of calixarene derivatives, and the values of surface coverage (θ) for different concentrations of P1and P2 in 1M HCl were evaluated from weight loss measurements using the equation [38]:

$$\theta = \frac{W_{corr} - W_{corr(inh)}}{W_{corr}} \qquad (8)$$

In order to get a better understanding of the electrochemical process on the metal surface, adsorption characteristics are also studied for calixarene derivatives. This process is closely related to the adsorption of the inhibitor molecules [39] and adsorption is known to depend on the chemical structure [40]. Adsorption isotherms are very important in determining the mechanism of organic electrochemical reactions. The most frequently used adsorption isotherms are Langmuir, Temkin and Frumkin.

In hydrochloric acid solution, the organic compound follows the Langmuir adsorption isotherm. This is as follows:

$$\frac{C}{\theta} = \frac{1}{K} + C \qquad (9)$$

Where C is the concentration of inhibitor, K is the equilibrium constant of the adsorption process, and □ is the surface coverage.

From the values of surface coverage, the linear regressions between C/Θ and C are calculated and the parameters (adsorption coefficients, slopes, and linear regression coefficients) are listed in Table 6. Fig. 6 shows the relationship between C/□□ and C at various temperatures. These results show that the linear regression coefficients (r) and the slopes are almost equal 1.000, indicating that the adsorption of inhibitor onto steel surface agrees the Langmuir adsorption isotherm. In addition, the equilibrium constant of the adsorption process (K) decreases with increasing temperature (Table 6). It is well known that K designates the adsorption power of inhibitor onto the steel surface; clearly, calixarene derivatives gives higher values of K at lower temperatures, indicating that it was adsorbed strongly onto the steel surface. Thus, the inhibition efficiency decreased slightly with the increase in temperature as the result of the improvement for the desorption of P1 and P2 from the steel surface. The corrosion inhibition of inhibitors for steel may be well explained by using thermodynamic model, so, the heat, the free energy and the entropy of adsorption are calculated to elucidate the phenomenon for the inhibition action of P1 and P2.

According to the Van't Hoff equation [41-44]:

$$\ln K = \frac{-\Delta H^{0}_{ads}}{RT} + constant \qquad (10)$$

where ΔH°_{ads} and K are the adsorption heat and adsorptive equilibrium constant, respectively. To obtain the adsorption heat, the linear regression between lnK and 1/T is dealt with, the relationship between lnK and 1/T is shown in Fig.7. Under the experimental conditions, the adsorption heat could be approximately regarded as the standard adsorption heat (ΔH_{ads}) [45]. The obtained value of ΔH_{ads} is -20.90 kJmol^{-1} for P1 and -26.26 kJmol^{-1} for P2. The standard adsorption free energy (ΔG_{ads}) is obtained according to the following equation [46]:

$$K = \frac{1}{55.5}\exp\left(\frac{-\Delta G^{0}_{ads}}{RT}\right) \quad (11)$$

The negative values of ΔG_{ads} (Table5) ensure the spontaneity of the adsorption process and stability of the adsorbed layer on the steel surface [47]. Furthermore, it is found that ΔG_{ads} slightly increases with temperature. The negative values of ΔH_{ads} also show that the adsorption of inhibitor is an exothermic process [48]. Generally, an exothermic process signifies either physi- or chemisorption while endothermic process is attributable unequivocally to chemisorption [49]. In an exothermic process, physisorption is distinguished from chemisorptions by considering the absolute value of a physisorption process is lower than 40kJmol^{-1} while the adsorption heat of a chemisorption process approaches 100kJmol^{-1} [50]. In the present case; the standard adsorption heat -20.90 kJmol^{-1}for P1 and -26.26 kJmol^{-1}for P2 shows that a comprehensive adsorption (physical adsorption) might occur [41]. The same results were obtained in previous studies [42].

ΔH_{ads} = -20.90 kJmol^{-1} for P1 and -26.26 kJmol^{-1} for P2 found by the Van't Hoff equation, may be also evaluated by the Gibbs–Helmholtz equation, which is defined as follows:

$$\left[\frac{\partial(\Delta G^{0}_{ads}/T)}{\partial T}\right]_{P} = -\frac{\Delta H^{0}_{ads}}{T^{2}} \quad (12)$$

which can be arranged to give the following equation:

$$\frac{\Delta G^{0}_{ads}}{T} = \frac{\Delta H^{0}_{ads}}{T} + A \quad (13)$$

The variation of $\Delta G_{ads}/T$ with 1/T gives a straight line with a slope that equals ΔH_{ads} (Fig.8). It can be seen from Fig. 8 that $\Delta G_{ads}/T$ decreases slightly with 1/T in a linear fashion. The values of ΔH_{ads} is negative (ΔH_{ads} = -20.90 kJmol^{-1} for P1 and -26.26 kJmol^{-1}for P2), reflecting the exothermic behaviour of adsorption on the steel surface. The value of the enthalpy of adsorption found by the two methods such as Van't Hoff and Gibbs–Helmholtz relations are in good agreement.

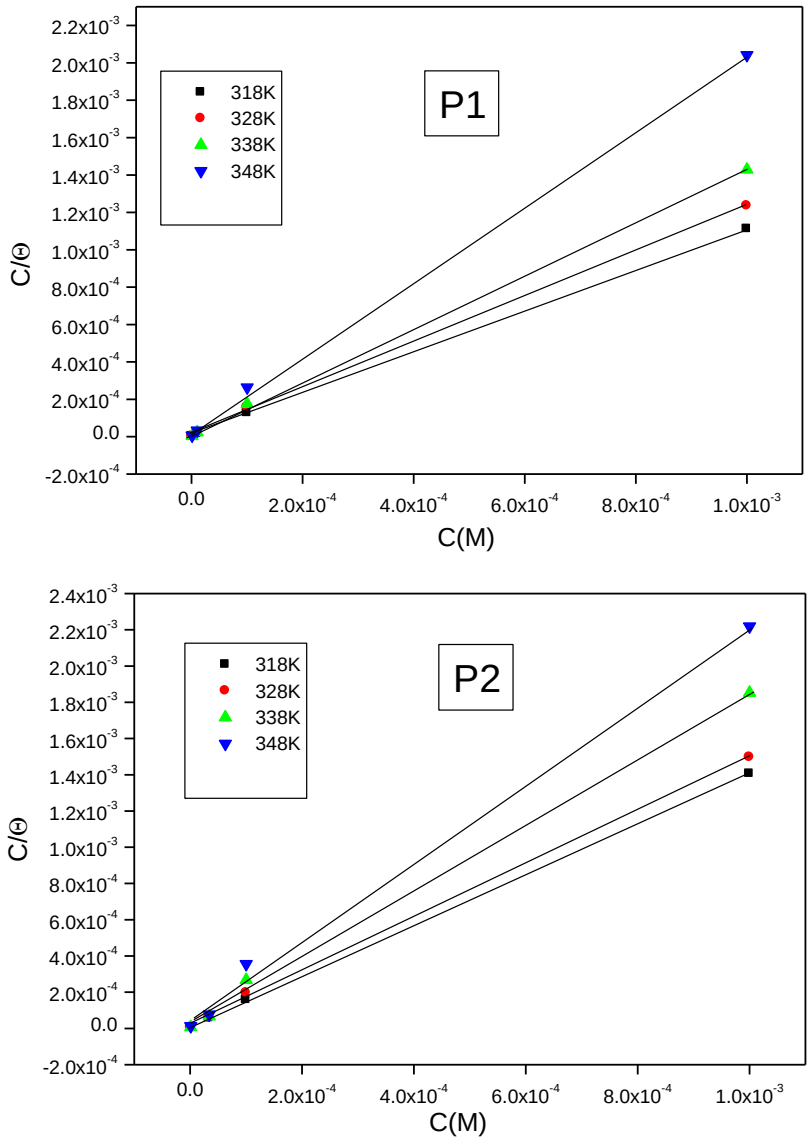

Figure 6. Langmuir adsorption plots for carbon steel in 1M HCl containing different concentrations of inhibitors at different temperatures.

Table 6. Adsorption parameters of the linear regression between C/ □ and C of P1and P2.

Inhibitor	T(K)	A	*K*	r	$\Delta G°_{ads}$ (kJ mol^{-1})	$\Delta H°_{ads}$ (kJ mol^{-1})	$\Delta S°_{ads}$ (J $mol^{-1}K^{-1}$)
P1	318	$5.96.10^{-6}$	$167.78.10^{3}$	1.06	-42.45		-67.67
	328	$1.29.10^{-5}$	$77.52.10^{3}$	1.07	-41.68	-20.93	-63.26
	338	$1.45.10^{-5}$	$68.965.10^{3}$	1.15	-42.62		-64.17
	348	$2.44.10^{-5}$	$40.98.10^{3}$	1.20	-42.38		-61.63
P2	318	$2.34.10^{-5}$	$42.73.10^{3}$	1.03	-38.83		-40.28
	328	$2.82.10^{-5}$	$35.46.10^{3}$	1.04	-39.54	-26.02	-41.22
	338	$3.53.10^{-5}$	$28.33.10^{3}$	1.08	-40.12		-41.71
	348	$5.70.10^{-5}$	$17.54.10^{3}$	1.12	-39.9		-39.88

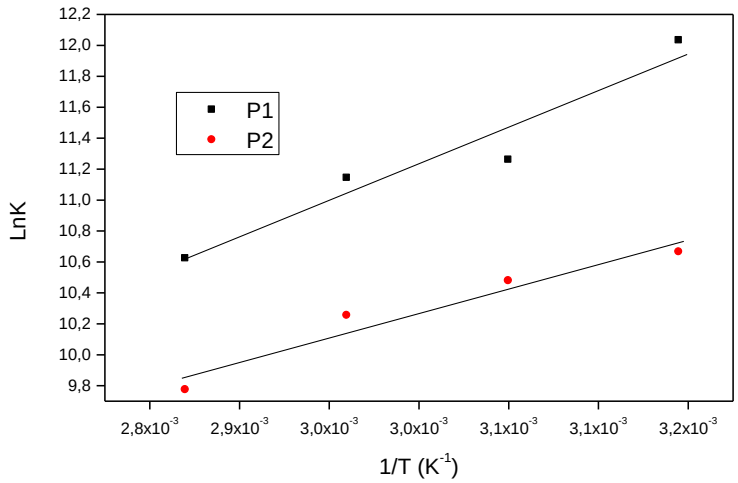

Figure 7. Variation of ln(K)with 1/T for mild steel in 1.0M HCl in the presence of inhibitors P1 and P2

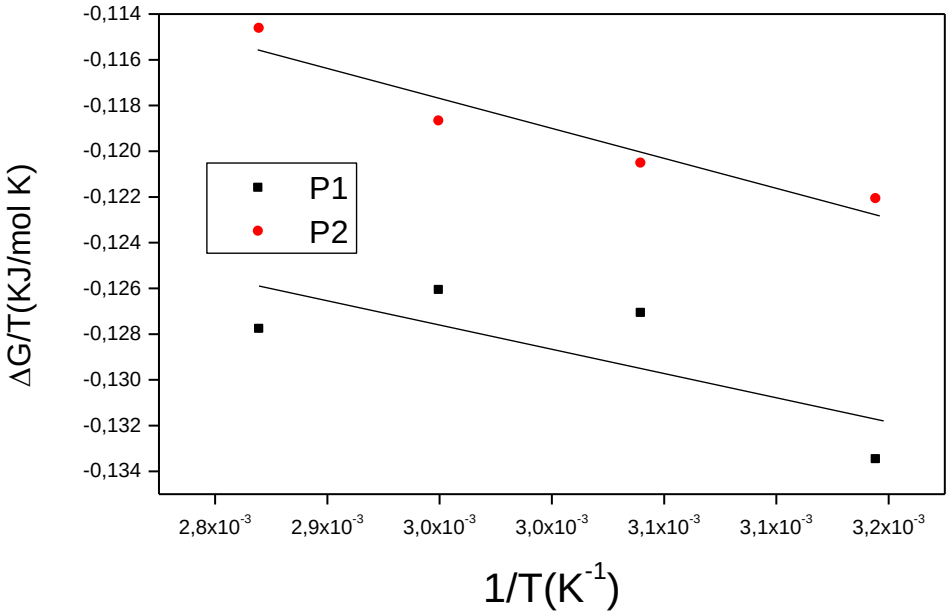

Figure 8. The relationship between ΔG°_{ads} and T

4. CONCLUSION

This influence of new synthesized calixarene derivatives namely calix[8]arenes (3a) (P1) and (2a) (P2) on the corrosion of steel in molar HCl conducted the following conclusions :

1. The inhibition efficiency increases with calixarene content to reach 95.14% for (P1) and 80% for (P2) at 10^{-3}M.

2. Polarization curves showed that P1 and P2 acted as mixed type inhibitors by decreasing current densities.

3. They adsorbed on the surface according to the Langmuir adsorption isotherm.

4. Free enthalpy of adsorption determination suggested that calixarene derivatives acted by physisorption onto the steel surface.

References

1. M. Bouklah, B. Hammouti, M. Lagrene, F. Bentiss, *Corros. Sci.* 48 (2006) 2831
2. M. Bouklah, B. Hammouti, A. Aouniti, M. Benkaddour, A. Bouyanzer, *Appl. Surf. Sci.* 252 (2006) 6236
3. M. Bouklah , B. Hammouti, *Port. Electrochim. Acta* 24 (2006) 457
4. O. Ouachikh, A. Bouyanzer, M. Bouklah, J-M. Desjobert, J. Costa. B. Hammouti, L. Majidi, *Surf. Rev. and Letters.* 16 (2009) 49.
5. F. Bentiss, M. Lagrenée, M. Traisnel, J.C. Hornez, *Corros. Sci.* 41 (1999) 789.
6. M. Dahmani, A. Et-Touhami, S.S. Al-Deyab , B. Hammouti, A. Bouyanzer, *Int. J. Electrochem. Sci.,* 5 (2010) 1060.
7. A. Zarrouk, I. Warad, B. Hammouti, A Dafali, S.S. Al-Deyab, N. Benchat, *Int. J. Electrochem. Sci.,* 5 (2010) 1516.
8. G. Moretti, G. Quartarone, A. Tassan, A. Zlngales. *Electrochim. Acta* 41 (1996) 1971.
9. F. Bentiss, M. Traisnel, M. Lagrenée, *Corros. Sci.*, 42 (2000) 127.
10. A. Chetouani, A. Aouniti, B. Hammouti, N. Benchat, T. Benhadda, S. Kertit, *Corros. Sci.* 45 (2003) 167.
11. H. Shokry, M. Yuasa, I. Sekine, R.M. Issa, H.Y. El-Baradie, G.K. Gomma, *Corros. Sci.* 40 (1998) 2173.
12. A.Yurt, A.Balaban, S.U Kandemir, G. Bereket, B. Erk. *Mater. Chem. Phys.* 85 (2004) 420.
13. H.Ju , Z.Kai, Y. Li. *Corros. Sci.* 50 (2008) 865–871.
14. I. Ahamad, R. Prasad, M.A. Quraishi, *Corros. Sci.* 52 (2010) 933.
15. C. D. Gutsche, Calixarenes (The Royal Society of Chemistry, Cambridge, 1992).
16. Z. Asfari, V. B¨ohmer, J. Harrowfield and J. Vicens (eds.), Calixarenes 2001 (Kluwer Academic Publishers, Dordrecht, The Netherlands, 2001).
17. J. Harrowfield and J. Vicens (eds.), Calixarenes in Nanochemistry (Springer, Dordrecht, The Netherlands, 2007).
18. L. Mandolini and R. Ungaro, Calixarenes in Action (Imperial College Press, London, England, 2000).
19. Wu Chong, Wen-Juan Zhang, Xi Zeng, Lan Mu, Sai-Feng Xue, Zhu Tao, Takehiko Yamato, *J. Incl. Phenom. Macro.* 66 (2010) 125.
20. C. Wieser, C. B. Deleman and D. Matt, *Coord. Chem. Rev.* 165 (1997) 93.
21. G. J. Lumetta and R. D. Rogers (eds.), Calixarenes for Separations, A. S. Gopalan, *ACS Symp. Series* 757 (2000).
22. R. Ludwig, *Fresenius J. Anal. Chem.* 367 (2000) 103.
23. L. Cecille, M. Carsarci and L. Pietrelli, New Separation Chemistry Techniques for Radioactive Wastes and Other Applications (Elsevier Applied Sciences, London, England, 1991).
24. F. Arnaud, M. J. Schwing-Weill and J. F. Dozol, in Calixarenes 2001, eds. Z. Asfari, V. B¨ohmer, J. Harrowfield and J. Vicens (Kluwer Academic Publishers, Dordrecht, The Netherlands, 2001), pp. 642–662.
25. R. Souane, M. Kaddouri, M. Bouklah, N. Cheriaa, B. Hammouti, J. Vicens, *Surface Review and Letters,* 16 (2009) 401

26. M. Kaddouri, N. Cheriaa, R. Souane, M. Bouklah, A. Aouniti, R. Abidi, B. Hammouti, J. Vicens, *J. Appl. Electrochem.* 38 (2008) 1253.
27. M. Benabdellah, R. Souane, N. Cheriaa, R. Abidi, B. Hammouti, J. Vicens, *Pigm. Resin Techn*. 36 (2007) 373.
28. Natalya V. Likhanova, Octavio Olivares-Xometl, Diego Guzmán-Lucero,
29. Marco A. Domínguez-Aguilar, Noel Nava1, Mónica Corrales-Luna, M. Consuelo Mendoza, *Int. J. Electrochem. Sci.,* 6 (2011) 4514
30. B.G. Ateya, B.M. Abo El-Khair, I.A. Abdel Hamid, *Corros. Sci.* 16, (1976)163
31. M. Bouklah, A. Ouassini, B. Hammouti, A. El Idrissi, *Appl. Surf. Sci.* 252, (2006) 2178
32. F .Bentiss, M. Lebrini, M. Lagrenee, *Corros. Sci.* 47, (2005) 2915
33. Z.Szklarska-Smialowska, Electrochemical, Optical Techniques for the study of Metallic Corrosion, Kluwer Academic Publishers, Dordrecht, 545 (1991)
34. J.O'M. Bockris, A.K.N. Reddy, Modern Electrochemistry, vol. 2, Plenum Press, New York, 1977. p. 1267.
35. I. El Ouali, B. Hammouti, A. Aouniti, Y. Ramli, M. Azougagh, E.M. Essassi, M. Bouachrine, *J. Mater. Environ Sci.,* 1 (2010) 1.
36. M. Bouklah, B. Hammouti, M. Lagrenée, F. Bentiss, *Corros. Sci.* 48 (2006) 2831
37. I.N. Putilova, S. A. Balezin, V. P. Barannik, Metallic Corrosion Inhibitors, Pergamon Press, Oxford, (1960).
38. S. Martinez, I. Stern, *Appl. Surf. Sci.* 199 (2002) 83
39. T. Tsuru, S. Haruyama, B. Gijutsu, *J. Jpn. Soc. Corros. Eng.* 27 (1978) 573
40. N.Hackerman, J.D.Sudbury. *J. Electrochem. Soc.*, 4 (1950) 94.
41. X.L.Cheng, H.Y.Ma, S.H.Chen, R.Yu, X. Chen, Z.M.Yao. *Corros. Sci.* 41, (1999) 321.
42. L.B.Tang, G.N.Mu, G.H Liu. *Corros. Sci.* 45, (2003) 2251.
43. B.Trachli, M.Keddam, H. Takenouti, A. Srhiri. *Prog. Org. Coat.* 44 (2002) 17.
44. X. Li, G.Mu. *Appl. Surf. Sci.* 252, (2005) 1254.
45. G.N. Mu, X.M. Li, F.Li. *Mater. Chem. Phys.* 86 (2004) 59.
46. T.P. Zhao, G.N. Mu. *Corros. Sci.* 41 (1999) 1937.
47. E.Khamis. *Corrosion* 46 (1990) 476.
48. S.A. Ali, A.M. El-Shareef, R.F. Al-Ghamdi, M.T.Saeed. *Corros. Sci.* 47, (2005) 2659.
49. G.K.Gomma, M.H. Wahdan. *Mater. Chem. Phys.* 39, (1995) 211.
50. W. Durnie, R.De Marco, B. Kinsella, A. Jefferson. *J. Electrochem. Soc.* 146 (1999) 1751.